FLEXURAL STRENGTHENING EFFECT OF RC BEAM BY HYBRID BONDING METHOD USING THERMOPLASTIC CFRP

Md. Golam MOSTOFA[1], Shinichi MIYAZATO[2] and Atsushi HOKURA[3]

[1]Graduate Student, Dept. of Civil and Environmental Eng., Kanazawa Institute of Technology
(3-1 Yatsukaho, Hakusan, Ishikawa, 924-0838, Japan)
E-mail: engr.mgm@gmail.com
[2]Member of JSCE, Professor, Dept. of Civil and Environmental Eng., Kanazawa Institute of Technology
(3-1 Yatsukaho, Hakusan, Ishikawa, 924-0838, Japan)
E-mail: miyazato@neptune.kanazawa-it.ac.jp
[3]Member of JSCE, Researcher, Innovative Composite Center, Kanazawa Institute of Technology
(2-2 Yatsukaho, Hakusan, Ishikawa, 924-0838, Japan)
E-mail: hokura@neptune.kanazawa-it.ac.jp

The application of conventional thermosetting carbon fiber reinforced polymer (CFRTS) is now becoming popular in the repair and rehabilitation of concrete infrastructure. However, it is not widely used due to its high cost. Thermoplastic CFRP (CFRTP) may be an alternative, cost-effective material with easy processability and exclusive bendability compared to CFRTS. Externally-bonded reinforcement (EBR) and near-surface mounted (NSM) techniques are two frequently preferred methods for strengthening the existing structure. This study investigated the CFRTP bar's applicability in the flexural behavior of reinforced concrete (RC) beam strengthened through the combined externally bonded and near-surface mounted technique (hybrid bonding method). This approach is preferred when any structure has a restricted cross-sectional width or needs extra flexural capacity that cannot be achieved by a particular method or material. However, in previous studies, this method was performed using CFRTS or steel bar, but few studies have been conducted on beam strengthening incorporating thermoplastic CFRP. A four-point bending test was carried out on six beams strengthened with CFRP bar as NSM reinforcement combined with CFRP fabric as EBR composite to observe the flexural strengthening effect. The test variables were the CFRTP strand rod and CFRTS NSM bar, the thickness of CFRP fabric (one and two layers), and the U-wrap end anchorage. First crack load, yield, and ultimate capacities, deflection, failure modes, cracking behavior, strain, and bending stiffness of the beams were evaluated based on the experimental results. The test results were compared with the CFRTS hybrid strengthened beams and showed that the CFRTP hybrid strengthened beams significantly enhanced the RC beams' serviceability performance and ultimate capacity.

Key Words: *CFRTS, CFRTP, Hybrid bonding, Flexural strengthening, Bending stiffness*

1. INTRODUCTION

To meet the requirement for sustainable development, strengthening existing infrastructure is often necessary to maintain serviceability demand and enhanced load-carrying capacity. Due to structural deterioration, aggressive surrounding environment, faulty design, and construction error, carbon fiber reinforced polymer (CFRP) has been used in the repair and rehabilitation field of concrete structures over the past decades due to its high strength-to-weight ratio, corrosion resistance, and low density. Though, the application of the conventional thermosetting carbon fiber reinforced polymer (CFRTS) is common in strengthening infrastructure, due to its high cost, it is not widely used mainly in developing countries. In this regard, thermoplastic carbon fiber reinforced (CFRTP) strand rod may be used as alternative, inexpensive material with easy processability and exclusive bendability compared to CFRTS[1) ~2)].

Thermoplastic carbon fiber reinforced polymer is (CFRTP) composed of thermoplastic epoxy as a matrix resin and carbon fiber material. Nakada et al.[3)] discussed the creep loading effect on the CFRTP

strand rod. Hokura et al.[1] conducted the tensile test under different environmental conditions, the adhesion test with concrete, and the RC beam bending test of CFRTP strand rod as an internal reinforcement.

There are mainly two methods available to strengthen existing structures such as externally bonded reinforcement (EBR) and the other is near-surface mounted (NSM) technique. The EBR method consists of one or more FRP laminates applied to the reinforced member's tension side, while the NSM technique consists of inserting FRP strips or rods into the concrete cover zone as done by pre-cut grooves and then filled with epoxy adhesives[4].

The NSM technique offers a high degree of strengthening enhancement, is less susceptible to premature debonding failure, improves fire safety, enhances protection against mechanical damage, aging consequences, and vandalism attacks[5]. Moreover, the EBR method usually shows premature debonding failure due to high interfacial shear stressed between the FRP and concrete substrate at the location of FRP curtailment[6].

Sometimes in the NSM system, the beam width may not be sufficiently wide enough to provide the required edge clearance and clear spacing between two adjacent NSM grooves, according to the previous studies[7]. This strengthening technique demands more concrete cover to create enough space to cut grooves without the risk of damaging the existing steel. Nonetheless, due to defective construction or several other reasons, many existing structures have less concrete cover, which is a significant challenge for this technique[8].

About these limitations, a hybrid bonding technique, which is a combination of the EBR and NSM method, may be suitable to mitigate their limitations reciprocally. This technique is preferred when any structure has a restricted cross-sectional width or needs extra flexural capacity that cannot be achieved by a particular method or material. Previous work on the hybrid strengthening technique was done by Rahman et al.[9] and Darain et al.[10] and others. However, in previous studies, the hybrid beam strengthening technique was performed using CFRTS or steel bar, but few studies had been performed using thermoplastic CFRP material. In this study, the hybrid bonding method was applied to RC beam specimens with a comparatively shorter span to depth ratio to justify the technique's application.

In the previous studies, It is observed that the reduction in a fabric thickness of Carbon Fiber Reinforced Polymer (CFRP) reduces the degree of stress concentration on the edge of the fabric[11]. Through the proper combination, the CFRP fabric thickness can be decreased by shifting a part of the appropriate area of CFRP fabric material from EBR to NSM technique or vice versa to get optimum benefit of the applied material and thus provide sufficient space for edge clearance and clear groove spacing which may help reduce the possibility of concrete cover separation failure[12)~14)].

This study investigated a hybrid bonding method for flexural strengthening the RC beam, which used thermoplastic CFRP (CFRTP) strand rod as NSM combined with thermosetting EBR CFRP fabric at beam soffit to develop a cost-effective strengthening solution that will increase the load-carrying capacity and the serviceability requirements of the structure. The effect of the variables such as CFRTP and CFRTS NSM bar, the thickness of the CFRP fabric (one and two layers), and the U-wrap anchorage were evaluated based on a four-point bending test. In addition, a comparative study had been carried out among specimens that were strengthened with thermoplastic and thermosetting CFRP bars.

2. EXPERIMENTAL PROGRAM

(1) Test matrix

The experimental program consisted of six specimens of the RC beam. The first beam was assigned as the control specimen, and the remaining beams were strengthened with the hybrid bonding method. **Table 1** summarizes the detailed test matrix. The primary test variables were NSM reinforcement diameter (8 mm and 9.3 mm), external thermosetting CFRP fabric thickness (one and two layers), and U-wrap

Table 1 Test matrix of experimental program.

Notation	Description of tested beams
CB	Control Beam (Without Strengthening)
HP9F1	1-9.3 mm Ø thermoplastic CFRP NSM strand rod: L=1300 mm and one layer of EBR CFRP fabric :1300 ×125×0.167 mm^3
HS8F1	1-8.0 mm Ø thermosetting CFRP NSM bar: L=1300 mm and one layer of EBR CFRP fabric:1300 × 125 × 0.167 mm^3
HP9F2	1-9.3 mm Ø thermoplastic CFRP NSM strand rod: L=1300 mm and two-layers of EBR CFRP fabric. EBR first layer fabric:1300 × 125 × 0.167 mm^3, EBR second layer fabric: 1000×125 × 0.167 mm^3
HP9F2A	1-9.3 mmØ thermoplastic CFRP NSM strand rod : L=1300 mm, two layers of EBR CFRP fabric: 1300 x 125 x 0.334 mm^3 and two-layers U-wrap end anchorage: 625×125 ×0.334 mm^3
HS8F2A	1-8.0 mm Ø thermosetting CFRP NSM bar: L=1300 mm, two layers of EBR CFRP fabric: 1300× 125× 0.334 mm^3 and two layers U-wrap end anchorage: 625 × 125 × 0.334 mm^3

end anchorage at the curtailment location of EBR fabric. There were also differences in the length of the EBR CFRP fabric. For the single-layer condition, a 1300 mm-long CFRP fabric was attached to the beam soffit. For the double-layer case, the second ply was 1000 mm length to avoid end peeling failure due to increased normal stress at the CFRP fabric's curtailment end [15]. The notation of the beam is outlined as follows, "HP9F2A" as an example where H denotes the hybrid bonding technique. P and S indicate thermoplastic and thermosetting NSM CFRP bar respectively, 8 and 9 denote 8 mm bar and 9.3 mm strand rod sequentially, F1 and F2 symbolize the single-layer and double-layer of CFRP fabric through the EBR technique, whereas A stands for U-wrap end anchorage.

(2) Specimen and materials

The cross-sectional dimensions of the RC beams in the experimental program was 125 mm × 250 mm, and the length was 1800 mm. The effective span and shear-span length were 1400 mm and 560 mm (one side), respectively. The shear span to depth ratio was taken as 2.64. To design as an under-reinforced RC beam and to initiate failure in a flexural state, the steel ratio ($\rho = As/bd$) was kept as low as 0.01. Two 13 mm and 10 mm diameter deformed bars were used as the bottom and top reinforcements, respectively, having a 6 mm diameter stirrup with a 45 mm spacing. A typical concrete clear cover of 25 mm was used. The top longitudinal and shear reinforcement were continued up to the experimental beam's shear span zone. Ready-mix concrete with a maximum aggregate size of 25 mm was used for concrete casting.

The mixture proportion of concrete is given in **Table 2**. The air content and slump value was 5.2 % and 19 cm, respectively. The same batch of concrete was used during casting for the six beams to keep the same concrete properties. The mechanical properties of concrete were evaluated at 28 days after concrete casting, such as compressive and flexural strengths, based on the cylinder (100 mm × 200 mm) and prism (400 mm× 100 mm× 100 mm) specimens. The properties of strengthened samples and materials are described in **Table 3**.

Either 9.3 mm φ thermoplastic CFRP strand rod or 8 mm φ thermosetting (area 50.2 mm^2) CFRP round bar was placed at the groove, which had a unit weight of 88 g/m and 94 g/m, respectively. The 9.3 mm φ CFRTP strand rod had an effective cross-sectional area of 27.5 mm^2 that carried the force of composite materials (different from the actual cross-sectional area) according to the manufacturer's specification.

Unidirectional CFRP fabric with a thickness of 0.167 mm was applied as EBR composite at the beam soffit level. In strengthened beams, the same CFRP fabric was used for the U-wrap end anchorage. A two-part epoxy resin adhesive (main agent and hardener) was used to attach the CFRP bar and CFRP fabric with concrete. Before application of epoxy resin adhesive, a two-part epoxy primer (main agent and hardener) was used in the concrete groove cutting and beam surface. Primer and epoxy adhesive was prepared according to manufactures' specification.

Table 2 Mix proportion of concrete.

W/C(%)	s/a(%)	Mix composition (kg/m^3)				
		W	C	S	G	Ad
44.8	45.1	167	373	775	960	2.61

Table 3 Properties of strengthened specimens and materials.

Material	Mechanical property	Result
Concrete	Compressive strength (Mpa)	43.86
	Flexure Strength (Mpa)	3.93
	Elastic Modulus (Gpa)	31.7
Steel 13 mm (SD345) (Internal bottom reinforcement)	Yield strength (MPa)	384
	Tensile Strength (Mpa)	552
	Elongation (%)	20
Steel 10 mm (SD345) (Internal top reinforcement)	Yield strength (MPa)	373
	Tensile strength(Mpa)	539
	Elongation (%)	23
Steel 6 mm (SD295A) (Internal shear reinforcement)	Yield strength (MPa)	411
	Tensile strength (Mpa)	534
	Elongation (%)	17
CFRTP strand rod (9.3 mm φ)	Tensile strength (kN)	≥80
	Elastic modulus (GPa)	160
	Ultimate strain (%)	1.82
CFRTS bar (8 mm φ)	Tensile strength (kN)	103.5
	Elastic modulus (GPa)	152
	Ultimate strain (%)	1.36
CFRP fabric (t = 0.167 mm)	Tensile strength (GPa)	3.4
	Elastic modulus (GPa)	230
	Ultimate strain (%)	1.48
Epoxy adhesive curing condition 20 ±1°C, 7 days	Compressive strength (Mpa)	≥70
	Tensile strength (MPa)	≥30
	Tensile shear strength (MPa)	≥12.5
Epoxy primer	Viscosity (mPa·s) (at 23°C)	400

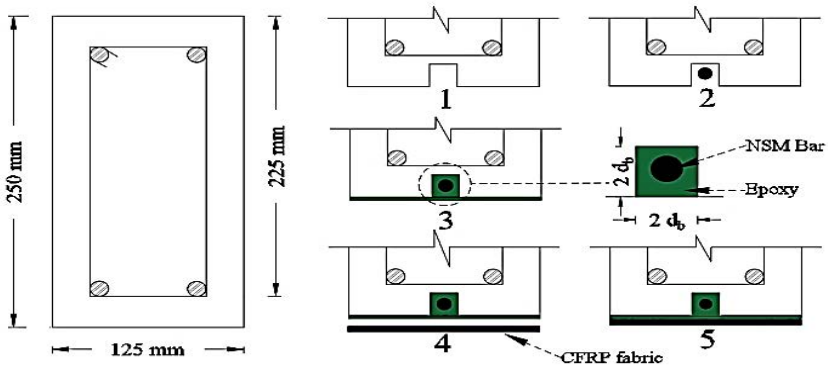

Fig. 1 Sequence of specimen preparation and hybrid-strengthening.

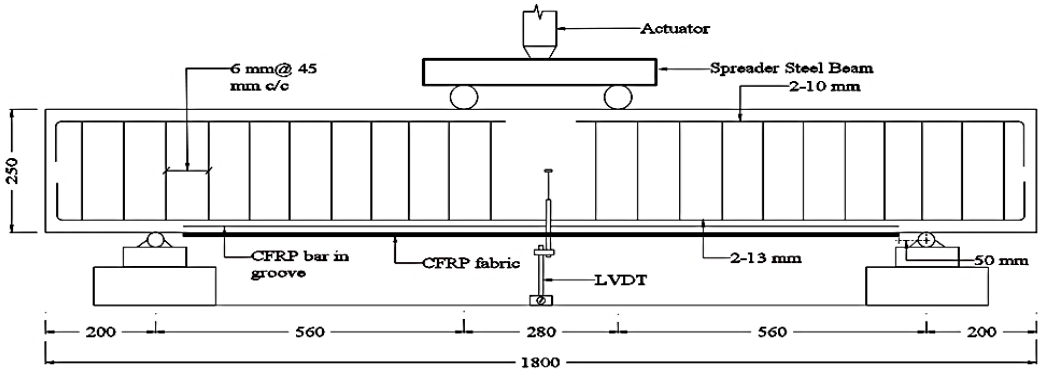

Fig. 2 Beam details and test setup (all dimensions are in mm).

(3) Strengthening procedure

The beam specimen preparation and strengthening processes are illustrated in **Fig 1**. A quality diamond-blade concrete cutter was used to create 18 mm ×18 mm and 16 mm ×16 mm groove at the tension face of the RC beam's longitudinal direction to accommodate the 9.3 mm strand rod and 8 mm diameter CFRP bars. The groove dimension was set as 2.0 d_b × 2.0 d_b (where d_b is the diameter of the NSM CFRP bar). The concrete groove lugs were taken out manually with a hand chisel and a hammer following the use of the concrete cutter. The cement laitance and loose materials of the concrete surface were removed with the help of a concrete grinder to ensure proper bonding of the concrete–EBR CFRP assemblage. The ground concrete surface was then cleaned to remove dust, loose particles, and any other foreign materials with the help of a wire brush and air pressure jet. Epoxy primer was applied to the groove and ground concrete surface before using epoxy resin and left the specimen for at least one day according to the manufacturer's recommendation. After the curing period, an approximately two-thirds portion of the groove was filled with epoxy resin.

Then, The NSM CFRP bar was adequately cleaned and gently pressed inside the groove until surrounded by an equal amount of epoxy. With the help of a brush and roller, the epoxy adhesive was spread over the surface, and then CFRP fabric was laid on it. A roller was pressed firmly on the fabric layer until the epoxy adhesive was squeezed out through the tiny pores of the CFRP fiber. To attach the second layer of CFRP fabric, epoxy was spread on the first fabric layer at the same time. Before the loading test, the sample was left at least seven days for curing time, as recommended by the manufacturer.

(4) Test setup

The beam details and test setup is presented in **Fig. 2**. All the beams were tested using a 1000 kN load-carrying capacity universal testing machine under a four-point bending test. In measuring the deflection at beam midspan, two linear variable displacement transducer (LVDT) was placed at the center of the maximum moment region and the average deflection was taken during the calculation. Before concrete casting, to attach the strain gauges with the rebar surface, the steel rebar surface was appropriately ground to remove the ribs. Acetone was used to clean the ground rebar surface. Two 3 mm-long strain gauges were mounted at the beam's midspan to measure the steel reinforcement strain on each internal steel rebar. For measurement of the NSM CFRP bar's strain value, the two 3 mm-long strain gauges were affixed at the central point, each of which was 25 mm away from the center of the strengthening bar. In the CFRP fabric, 3 mm-long strain gauges were

installed at the center point, 250 mm and 500 mm away from the central point of the EBR composite. The 60 mm-long strain gauges were positioned at the uppermost surface of the beam specimen to measure concrete compressive strain. Several 60 mm long strain gauges were attached to measure transverse strain along with the mid-span depth of the beam. All the data of the static load test were recorded using a load control condition.

3. RESULT AND DISCUSSION

(1) Load-carrying capacity

The experimental results of the hybrid strengthened RC beams are summarized in **Table 4**. These beams were strengthened with the thermoplastic or thermosetting CFRP bar inside the NSM groove and CFRP fabric affixed at the beam soffit. The test variables were the bar diameter (8 mm and 9.3 mm), the thickness of the CFRP fabric layer (one and two layers), and the U-wrap end anchorage (with and without) at the cut-off point of the EBR CFRP fabric. Results were expressed in terms of their first crack load, yield load, and ultimate load-carrying capacity and corresponding displacement.

The experimental results showed that hybrid strengthening with thermoplastic CFRP bar (HP9F1, HP9F2, and HP9F2A) showed gradually increased load-carrying capacity at any load level because of the additional second layer of EBR fabric at beam soffit and end anchorage application. Moreover, the HS8F1 beam showed a higher load-carrying capacity than HP9F1 because of CFRTS NSM bar had about 29 % higher tensile strength than the CFRTP NSM strand rod.The HS8F2A beam showed a maximum of 181 kN load-carrying capacity than all other hybrid strengthened beams. The results of the percentage increment of first crack load, yield load, ultimate load-carrying capacity compared with the control beam can be observed in **Fig. 3**. The increment of the first crack load of strengthened beams ranged from 43% to 186%, and the average increment was 99% more

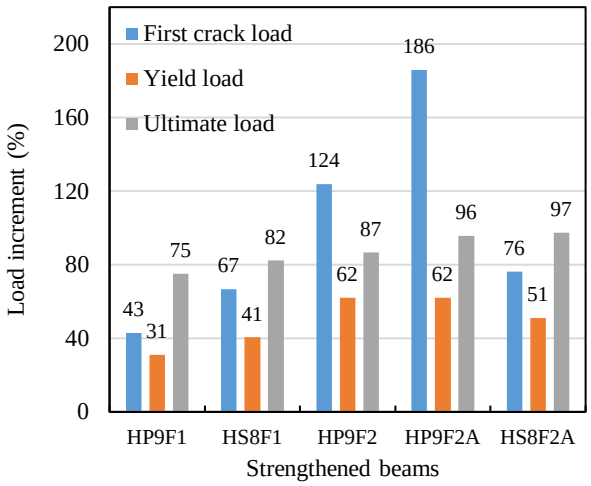

Fig. 3 Percentage increment of load carrying capacities of strengthened beams compared with control beam.

compared to that of the control beam, which was the maximum load increment at any load level. The yield load increment of the strengthened beams ranged from 31% to 62% compared to the control beam. Strengthened beams average increment of the ultimate load-carrying capacity was about 87 % compared to the control beam. Hybrid strengthened beams with thermoplastic NSM strand rod showed better performance in the first crack load and ultimate load compared with the control beam.

(2) Load-deflection behavior

The load versus midspan deflection curves for specimen beams are plotted in **Fig.4**. All the hybrid-strengthened RC beams exhibited almost trilinear response up to the ultimate load. The first portion of the curve up to crack load followed a linear elastic shape identical to the control beam, which resulted from the contribution of concrete, internal steel, and strengthening material together. The strengthened beams' first crack load varied from 30 kN to 60 kN, whereas deflection ranged from 2.42 mm to 5.0 mm. The second segment was the post-crack stage up to the yield point of the internal steel. At this portion, strengthened beams showed stiffness enhancement compared with the control beam.

Table 4 Summary of experimental beam test results.

Beam ID	P_{cr} (kN)	Δ_{cr} (mm)	P_y (kN)	Δ_y (mm)	P_u (kN)	Δ_u (mm)	Failure modes
CB	21	1.15	74	7.67	92	22.33	FFC
HP9F1	30	2.42	97	9.71	161	22.86	FFC
HS8F1	35	2.52	104	9.58	168	20.06	CS
HP9F2	47	3.60	120	10.49	172	17.26	CS
HP9F2A	60	5.00	121	11.00	180	19.63	CS
HS8F2A	37	2.75	112	10.19	181	20.52	CS

P_{cr} = first crack load; Δ_{cr} = deflection at first crack; P_y = yield load; Δ_y = deflection at yield of steel; P_u = ultimate load; Δ_u = mid-span deflection at failure load; FFC = flexural failure (concrete crushing after steel yielding); CS = concrete cover separation.

The third stage of the load-deflection curve continued from steel yielding to failure of the beam. After internal steel yielding, the NSM bar and EBR fabric controlled the deflection, cracking behavior, and load-carrying capacity until the specimen's failure. The strengthened beam demonstrated about 111% more average pre-ultimate stiffness enhancement compared with the control beam. The HP9F2-strengthened beam displayed a maximum of 141% more pre-ultimate stiffness relative to the control beam. However, the anchored HP9F2A strengthened beam demonstrated about 122% more pre-ultimate stiffness than the control beam. The strengthened beams performed a sudden drop of load-carrying capacity after reaching the post-peak response of the load-deflection curve, regardless of the failure modes.

Percentage deflection reduction (Δ_{rd}) of the strengthened specimens compared to the control beam at different load levels, such as 42 kN, 74 kN, and 92 kN load, can be observed in **Fig.5**. The last two loads were the yield and ultimate loads of the control beam. A 42 kN service load was taken for better comparison, which was the average first crack load of the strengthened beams.

The figure showed that the deflection was significantly reduced at different load levels. However, at 92 kN load, the difference was more noticeable than the other load level. At this load point, the deflection reduction was 59% to 65% in strengthened beams. The strengthened beams exhibited an average of 15% deflection reduction compared to the control beam, both in 42 kN and 74 kN load. Moreover, observing the data from the **Fig.5,** it could be supposed that the thermoplastic hybrid strengthened beam (HP9F1, HP9F2, and HP9F2A) showed improved performance in deflection reduction compared to the control beam at any load level.

(3) Modes of failures

The failure modes of all the experimental beams are shown in **Fig. 6**. The control beam failed typically by concrete crushing after steel yielding. The HP9F1 strengthened beam showed a similar type of flexure failure due to concrete crushing in compression after steel yielding but not as ductile as the control beam. All other strengthened beams (HS8F1, HP9F2, HP9F2A, and HS8F2A) exhibited premature debonding like concrete cover separation from the internal steel level as a brittle mode failure. The concrete cover separation was seen in the HP9F2A and HS8F2A beam specimens, though they were strengthened with U-wrap end anchorage. So, it could be mentioned that the application of U-wrap end anchorage (HP9F2A and HS8F2A) did not avoid concrete cover separation failure in hybrid strengthened beams where the shear span to depth ratio is comparatively shorter.

At first, the experimental beam generated a fine flexural crack in the midspan. As the external load increased, additional cracks were seen and propagated to the neutral axis or beyond the neutral axis, with a notable increase in the deflection of the beam. However, all the strengthened beam specimens showed distributed finer cracks with closer spacing compared to the control beam. It was due to the higher stiffness of the strengthened beam specimens. After the yielding of the internal steel reinforcement, a shear crack initiated at the end of the curtailment point of EBR fabric and the existing cracks width rapidly increased. Before the ultimate load, some new cracks were launched from the bottom soffit of beam at shear zone, which was a sign of high tensile and bond shear stresses development at the FRP-concrete interface. These new cracks widened rapidly and propagated along horizontally, and the ultimate failure of the strengthened beam specimens occoured.

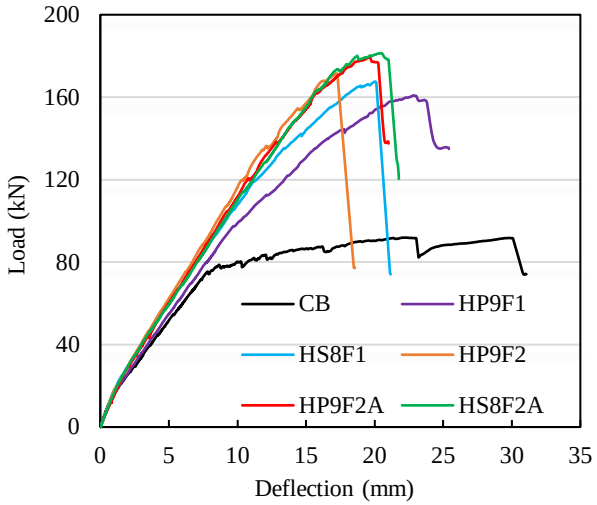

Fig.4 Load-deflection diagram at midspan of beams.

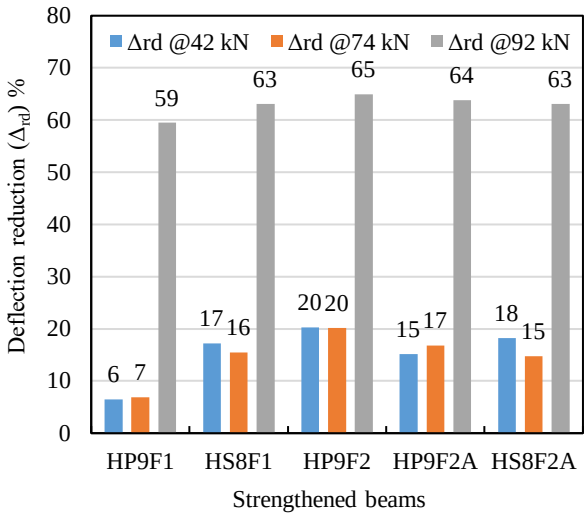

Fig.5 Percentage deflection reduction (Δ_{rd}) of strengthened beams compared with control beam at different load.

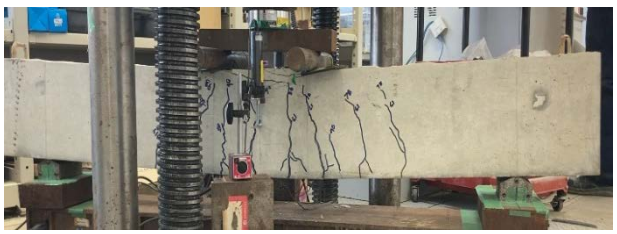

(a) CB

(b) HP9F1

(c) HS8F1

(d) HP9F2

(e) HP9F2A

(f) HS8F2A

Fig. 6 Failure modes of beam specimens.

(4) Cracking behavior

During the test, cracking behavior was monitored. The first crack was observed with the naked eye, and subsequent primary crack width, crack spacing, crack nos. were measured at the main internal reinforcement level in different loads by the crack scale and tape measure. The maximum, mean, and minimum crack spacing were determined based on the recorded data summarized in **Table 5**.

The maximum, minimum, and average crack spacing of hybrid-strengthened beams was comparatively lower than that of the control beam. This information confirmed the better energy dissipation of the hybrid strengthened beams.

Table 5 Crack spacing and crack nos. in beam specimens

Beam ID	$S_{r.max}$ (mm)	$S_{r.min}$ (mm)	$S_{r.mean}$ (mm)	No. cracks
CB	172	48	93	10
HP9F1	117	13	48	27
HS8F1	125	10	53	22
HP9F2	171	15	54	24
HP9F2A	82	12	48	22
HS8F2A	78	16	39	25

$S_{r.max}$ = maximum crack spacing; $S_{r.min}$ = minimum crack spacing; $S_{r.mean}$ = average crack spacing.

The maximum and minimum crack spacing of the hybrid strengthened beams were observed 171 mm and 10 mm, respectively. The average crack spacing of the strengthened specimens maintained a range from 39 to 54 mm, whereas it was found 93 mm in the control beam.

The number of cracks that appeared in the strengthened beam was almost the same, and its average was about 24, compared with 10 number of cracks of the control beam. The HS8F2A-strengthened beam exhibited the maximum number of cracks (25 cracks), whereas the HS8F1 and HP9F2A-strengthened beam showed the minimum number of cracks (22 cracks). The strengthened beams displayed many cracks with a small width; in contrast, the unstrengthened control beam had fewer cracks with a large width. From the tabular data, it could be believed that the thermoplastic hybrid strengthed beams showed similar cracking behavior compared to the thermosetting hybrid strengthened beams.

(5) Concrete compressive strain

The relationship between load and concrete compressive strain at the top concrete fiber at mid-span of the experimental beams is presented in **Fig.7**. The hybrid strengthened beam specimens demonstrated less concrete compressive strains than the control

beam because of the hybrid strengthened beams' higher stiffness.

Replacing the thermoplastic NSM CFRP strand rod with a higher tensile strength thermosetting CFRP bar in the beam specimen resulted in an increase in the HS8F1 beam's stiffness compared with the HP9F1 specimen at any load level. On the contrary, the HP9F2A specimen exhibited higher compressive strain than the HP9F2 specimen as U-warp end anchorage was attached to the HP9F2A specimen.

(6) CFRP tensile strain

The tensile strain of internal steel, NSM bar, EBR CFRP fabric was observed in the experimental program. The tensile strain of EBR CFRP fabric at midspan of strengthened beams is displayed in **Fig.8**. The strain of EBR CFRP fabric showed that the HP9F2 strengthened beam confirmed more stiffness than the HP9F1 because of the additional second layer of CFRP fabric attached to the HP9F2. Besides, the HP9F1 beam demonstrated the highest tensile strain, and the HP9F2 beam showed the lowest tensile strain than any other strengthened beam at any load level.

Fig.9 summarizes the tensile strain utilization (ratio of experimental strain and ultimate strain) ratio of CFRP NSM bar and EBR fabric at midspan and ultimate load level. HP9F1 strengthened beam demonstrated maximum use of CFRP tensile strain as EBR and NSM as strengthening material. The strain utilization ratio decreased in the HP9F2 beam as the area of EBR material increased. Again, the CFRP utilization ratio increased in the HP9F2A than the HP9F2 strengthened beam because of the attachment U-wrap end anchorage that helped increase the strengthened beam ductility. However, the HS8F1 beam showed less CFRP utilization ratio compared to HP9F1 as the HS8F1 beam demonstrated premature debonding failure.

(7) Bending stiffness of the experimental beam

The bending stiffness was computed experimentally by applying the following equation.

$(EI)_{exp} = \frac{M}{\varphi}$ Where $M = \frac{P}{2} L_a$ and $\varphi = \frac{\varepsilon_c + \varepsilon_s}{d}$

M =Bending moment (kN-m),
P = Applied load (kN), L_a =Distance between the loading point and support (m),
φ =Curvature (m^{-1}), d = depth of the rebar (m),
ε_c = Top fiber concrete compression strain,
ε_s = Strain in internal tension-steel or CFRP bar

Fig.10 shows the bending stiffness of the strengthened beam. Bending stiffness of specimens was computed from internal steel strain. However, the bending stiffness of the HS8F1 beam was computed from

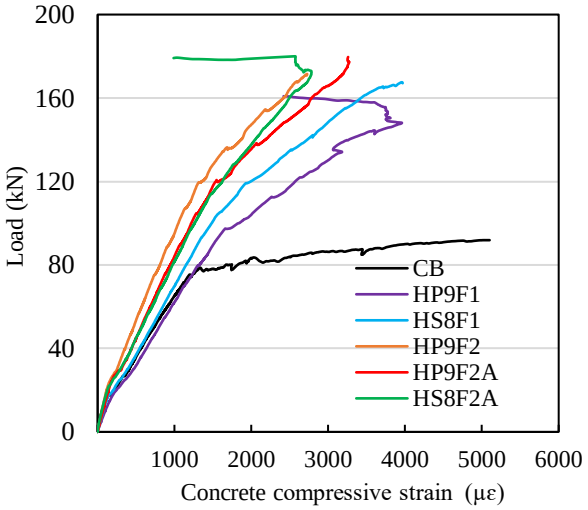

Fig. 7 Load *vs.* concrete compressive strain at midspan of the experimental beams.

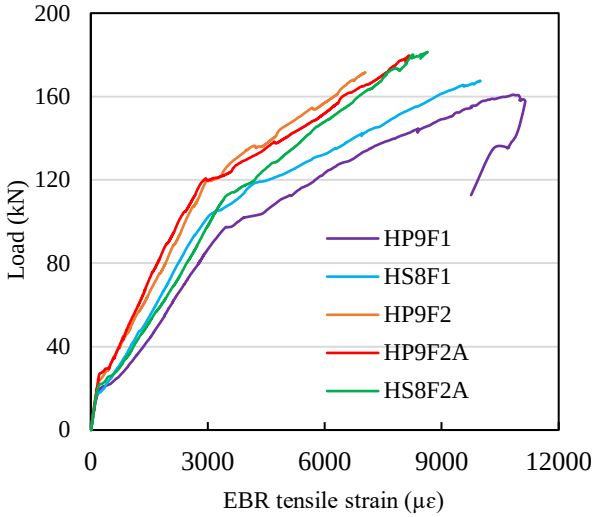

Fig. 8 Load *vs.* EBR CFRP tensile strain at midspan of the strengthened beams.

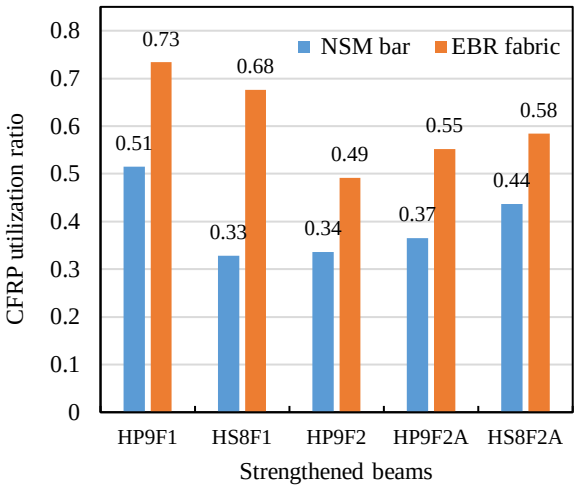

Fig. 9 CFRP utilization ratio at midspan of the strengthened beams.

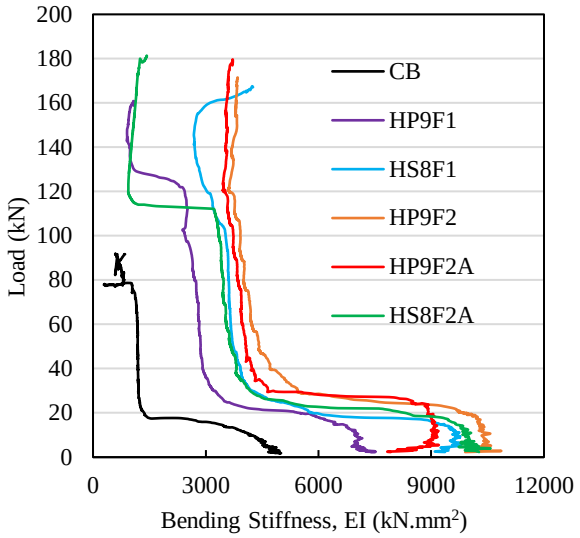

Fig. 10 Bending stiffness of experimental beams.

the CFRP NSM bar strain as the internal steel strain gauge was not working during the experiment. The overall shape of the load versus bending stiffness curve was formed like an "L" shape. The stiffness was initially high and then constantly decreased until the first crack appeared in the beam. No remarkable difference in stiffness was observed after the first crack, and a radical realignment was visualized. Moreover, after the yielding of internal steel reinforcement, the strengthened beams did not follow similar shape or pattern of bending stiffness curve.

For all cases, the hybrid strengthened beams exhibited an enhanced load-bending stiffness relationship compared with the control beam. The figure shows that applying additional EBR material area from one layer to two layers (HP9F1 and HP9F2) increased the bending stiffness of strengthened specimens. Bending stiffness also increased when higher strength CFRTS bar was used and replaced the lower strength CFRTP strand rod in the hybrid strengthened specimen (HP9F1 and HS8F1). However, the application of U-wrap end anchorage in an existing configuration decreased the stiffness of the strengthened beams (HP9F2 and HP9F2A).

The initial bending stiffness of the control beam was 5702 KN.mm^2. Whereas, the HP9F1, HS8F1, HP9F2, HP9F2A and HS8F2A strengthened beams showed initial bending stiffness of 7650, 9787, 10863, 9201, 10818 kN.mm^2, successively. The bending stiffness at first crack, yield load, and ultimate load level of the control beam was 1317,1105 and 591 kN.mm^2, respectively. The HP9F2 beam demonstrated maximum bending stiffness at first crack, yield, and ultimate load level than any other strengthened beams of 4455, 3615, and 3847 kN.mm^2, respectively.

4. CONCLUSION

This study investigated the flexural strengthening performance of the hybrid bonding method on RC beams, considering a comparatively shorter span to depth ratio. Using a thermoplastic CFRP (CFRTP) strand rod as an NSM bar combined with CFRP fabric at beam soffit was expected to develop a cost-effective strengthening solution. The effect of the variables such as the CFRTP and thermosetting CFRP (CFRTS) NSM bar, the thickness of the CFRP fabric, and U-wrap end anchorage performance were evaluated based on a four-point bending test. The flexural capacity, deflection, failure modes, cracking behavior, strain, and bending stiffness of the beams were analyzed.

The following summary can be drawn from the experimental outcomes:

- A trilinear load-deflection response was noticed up to the ultimate load of the strengthened beams. The first crack load, yield load, and ultimate load were significantly increased compared with the control beam. The average increment of the hybrid strengthened beams' first crack load was the highest (99%) among the three load levels, which is particularly essential for the serviceability requirement.
- The strengthened beams exhibited a considerable deflection reduction at the ultimate load level of the control beam specimen.
- All of the strengthened beams showed premature debonding failure like concrete cover separation, except the HP9F1 beam specimen demonstrating flexure failure by concrete crushing after steel yielding. However, concrete cover separation (HP9F2A, HS8F2A) was not eliminated by using U-wrap end anchorage.
- Increased total crack numbers and decreased crack spacing compared with the control beam ensured the hybrid strengthened beams' enhanced energy dissipation using thermoplastic CFRP.
- The thermoplastic strengthened beam HP9F1 demonstrated the highest CFRP strain utilization ratio than other strengthened beams, which indicated the optimum use of CFRP composites.
- The bending stiffness of the strengthened beam specimens significantly increased at all load levels than the control beam. Applying additional EBR composite area from one layer to two layers (HP9F1 and HP9F2) increased the stiffness of hybrid strengthened specimens.

Bending stiffness also increased when higher strength CFRTS NSM bar replaced lower strength CFRTP strand rod in the hybrid strengthened specimen (HP9F1 and HS8F1). However, the application of U-wrap end anchorage in an existing specimen decreased the bending stiffness of the strengthened beam (HP9F2 and HP9F2A).

- The experimental results showed that the hybrid bonding method could be applied in beam specimens where the shear span to depth ratio is comparatively shorter.
- The thermoplastic CFRP strand rod could be applied to the RC beam using a hybrid bonding method. It showed a similar type of load-carrying capacity, deflection, failure modes, and bending stiffness behavior compared to the hybrid strengthened beams using the thermosetting CFRP bar.

ACKNOWLEDGMENT: This study work was supported by JST COI Grant Number JPMJCE1315. Also, the authors gratefully acknowledge the assistance of Miyazato laboratory's students who helped during testing of the experimental program.

REFERENCES

1) Hokura, A. and Miyazato, S. : Feasibility study on thermoplastic FRP rod to rebar in concrete, *Journal of the Society of Materials Science*, Vol. 69, No. 4, pp. 335-342, 2020.
2) Mochida, Y. and Imoto, Y. : Development of carbon fiber reinforced thermoplastic strand rod, *International Journal of GEOMATE*, Vol. 16, pp. 109-115, 2019.
3) Nakada, M., Miyano, Y., Morisawa, Y., Nishida, H., Hayashi, Y. and Uzawa, K. : Prediction of statistical life time for unidirectional CFRTP under creep loading, *Journal of Reinforced Plastics and Composites*, Vol. 38, pp. 938-946, 2019.
4) De Lorenzis, L. and Teng, J. G.: Near-surface mounted FRP reinforcement: An emerging technique for strengthening structures, *Compos. B Eng.*, Vol. 38, No. 2, pp. 119–143, 2007.
5) Rosenboom, O. and Rizkalla, S.: Behavior of prestressed concrete strengthened with various CFRP systems subjected to fatigue loading, *J. Compos. Constr*, Vol. 10, No. 6, pp. 492–502, 2006.
6) Lousdad, A., Megueni, A. and Bouchikhi, A. S.: Geometric edge shape based optimization for interfacial shear stress reduction in fiber reinforced polymer plate retrofitted concrete beams, *Comput. Mater. Sci.*, Vol. 47, pp. 911-918, 2010.
7) Hassan, T. K. and Rizkalla, S. H.: Bond Mechanism of near-surface-mounted fiber-reinforced polymer bars for flexural strengthening of concrete structures, *Structural Journal*, Vol.101, No.6, pp.830-839, 2004
8) Park, Y., Kim, Y. H., and Lee, S-H.: Long-term flexural behaviors of GFRP reinforced concrete beams exposed to accelerated aging exposure conditions., *Polymers*, Vol. 6, No.6, pp. 1773–1793, 2014.
9) Rahman, M. M, Jumaat M. Z., Rahman, M. A. and Qeshta. M. I.: Innovative hybrid bonding method for strengthening reinforced concrete beam in flexure, *Construction and Building Materials*, Vol. 79, pp. 370-378, 2015.
10) Darain, K. M., Jumaat M. Z., Shukri, A.A., Obaydullah, M., Huda, M. N., Hosen, M. A. and Hoque, N.: Strengthening of RC beams using externally bonded reinforcement combined with near-surface mounted technique, *Polymers*, Vol. 8, 2016.
11) Arduini, M. and Nanni, A.: Parametric study of beams with externally bonded FRP reinforcement, *ACI Struct. J.*, Vol. 94, No.5, pp. 493–501, 1997.
12) Lim, D. H.: Combinations of NSM and EB CFRP strips for flexural strengthening of concrete structures, *Mag. Concr. Res*, Vol. 61, No.8, pp. 633–643, 2009.
13) Kotynia, R. and Cholostiakow, S.: New proposal for flexural strengthening of reinforced concrete beams using CFRP T-shaped profile, *Polymers*, Vol. 7, No. 11, pp. 2461–2477, 2015.
14) Rahman M. M., Structural hybridization and economical optimization of strengthening systems used for concrete beams. Ph.D. Thesis, Faculty of Engineering, University of Malaya, Kualalumpur, Malaysia, 2016.
15) Maalej. M. and Bian, Y.: Interfacial shear stress concentration in FRP-strengthened beams, *Compos. Struct.*, vol. 54, No. 4, pp.417–426, 2001.
16) Hosen, M.A., Jumaat, M.Z., Alengaram, U.J., Islam, ABMS and Hashim, H.B.: Near Surface Mounted Composites for Flexural Strengthening of Reinforced Concrete Beams. *Polymers*, Vol.*8*, No. 67, 2016.
17) Slaitas, J., Daugevičius, M., Valivonis, J. and Grigorjeva, T: Crack width, and load-carrying capacity of RC elements strengthened with FRP, *International Journal of Polymer Science*, Vol. 2018, Article ID 6274287, 2018.
18) El-Tahan, M., Galal, K. and Hoa, V. S.: New thermoplastic CFRP bendable rebars for reinforcing structural concrete elements, *Composites Part B: Engineering*, Vol. 45, No. 1, pp. 1207-1215, 2013.
19) Grelle, S.V. and Sneed, L. H.: Review of anchorage systems for externally bonded FRP laminates, *International Journal of Concrete Structures and Materials*, Vol.7, No.1, pp.17–33, 2013.
20) Huang, X., Sui, L., Xing, F., Zhou, Y. and Wu, Y: Reliability assessment for flexural FRP-Strengthened reinforced concrete beams based on Importance Sampling, *Composites Part B: Engineering*, Vol. 156, pp. 378-398, 2019.
21) Zhang, S.S., Yu, T. and Chen. GM: Reinforced concrete beams strengthened in flexure with near-surface mounted (NSM) CFRP strips: Current status and research needs, *Composites Part B*: Engineering, Vol. 131, pp 30-42, 2017.
22) Kalayci, A. S., Yalim, B. and Mirmiran, A.: Construction tolerances and design parameters for NSM FRP reinforcement in concrete beams, *Construction and Building Materials*, Vol. 24, No.10, pp.1821-1829, 2010.

(Received August 28, 2020)